
STRUCTURE NOTE

The 1.6-Å Resolution Crystal Structure of NovW: A 4-Keto-6-Deoxy Sugar Epimerase from the Novobiocin Biosynthetic Gene Cluster of *Streptomyces spheroides*

Piotr Jakimowicz¹ Mónica Tello,^{2,3} Caren L. Freel Meyers,⁴ Christopher T. Walsh,⁴ Mark J. Buttner¹ Robert A. Field,³ and David M. Lawson^{2*}

¹Department of Molecular Microbiology, John Innes Centre, Norwich, United Kingdom

²Department of Biological Chemistry, John Innes Centre, Norwich, United Kingdom

³Centre for Carbohydrate Chemistry, University of East Anglia, Norwich, United Kingdom

⁴Department of Biological Chemistry and Molecular Pharmacology, Harvard Medical School, Boston, Massachusetts

Introduction. The aminocoumarin antibiotics novobiocin, clorobiocin, and coumermycin A₁ are *Streptomyces* natural products. Despite their potency against Gram-positive bacteria, only novobiocin has seen limited clinical use because of toxicity problems and poor pharmacokinetics.¹ In recent years, however, there has been renewed interest in this family of compounds as potential lead molecules for the development of agents to combat multidrug resistant bacteria such as methicillin-resistant *Staphylococcus aureus*.^{2,3} Moreover, research on these compounds has been stimulated by the sequencing of the gene clusters encoding their biosynthetic pathways,^{4–6} as well as the development of powerful molecular biological tools for their manipulation.^{7–10}

The mode of action of the aminocoumarin antibiotics is well understood: they inhibit DNA gyrase,¹¹ an essential enzyme in bacteria and a validated drug target.^{1,12} They are competitive inhibitors of the adenosine triphosphatase (ATPase) reaction that drives the negative supercoiling of DNA, a process that must occur ahead of prokaryotic replication and transcription. Previous structural studies have shown the molecular basis for their action: the aminocoumarin binding site overlaps that for ATP in the B subunit.^{13–15} Two features are common to all three aminocoumarins, namely, the aminocoumarin ring and a noviose sugar. The latter moiety is responsible for the majority of the interactions with DNA gyrase and shows the most significant overlap with the ATP binding pocket. Noviose is an unusual 6-deoxy sugar that is derived from glucose-1-phosphate through the action of five gene products: a nucleotidyl transferase, a dehydratase, an epimerase, a methyltransferase, and a reductase. In novobiocin production, these enzymes are encoded by the products of the *novV*, *novT*, *novW*, *novU*, and *novS* genes, respectively, from *Streptomyces spheroides*.⁴ This pathway shows significant similarities with the well-studied rhamnose biosynthetic pathway,¹⁶ although there is no methyltransferase step in the latter. In particular, NovW is highly homologous to RmlC, the 4-keto-6-deoxy sugar epimerase. Until very

recently, two issues remained unaddressed concerning noviose biosynthesis. First, the ordering of the epimerization and methyltransfer steps had not been established, and second, it had not been shown whether there was a single or a double epimerization. However, a recent mechanistic study performed on NovW, NovU, and NovS suggested that NovW, like RmlC, is a 3,5-epimerase and that epimerization precedes methyltransfer.¹⁷ Herein, we describe the structure of NovW, which we have determined as part of a multidisciplinary study toward fully resolving these issues.

Materials and Methods. Crystals of NovW were obtained and cryoprotected as described previously.¹⁸ X-ray data were recorded to a maximum resolution of 1.6 Å at a temperature of 100 K on station PX9.6 ($\lambda = 0.870$ Å) at the Synchrotron Radiation Source in Daresbury (UK), using an Area Detector Systems Corporation Quantum 4 CCD detector. The resultant data were scaled and merged using the *HKL* package¹⁹ and all subsequent downstream processing and statistical analysis was effected using programs from the *CCP4* suite.²⁰ X-ray data collection parameters are summarized in Table I. Given that the crystals were isomorphous with the crystals obtained previously¹⁸

Grant sponsor: Biotechnology and Biological Sciences Research Council; Grant sponsor: National Institutes of Health; Grant numbers: F32 AI054007, GM 49338BBSRC; Grant sponsor: the Norwich Research Park; Grant sponsor: the Weston Foundation.

P. Jakimowicz's present address is Department of Microbiology, Institute of Immunology and Experimental Therapy, Polish Academy of Sciences, Weigla 12 Wrocław, PL-53-114, Poland.

C.L. Freel Meyers' present address is Department of Pharmacology and Molecular Sciences, Johns Hopkins University School of Medicine, Baltimore, MD 21205.

*Correspondence to: David M. Lawson, Department of Biological Chemistry, John Innes Centre, Norwich NR4 7UH, UK. E-mail: david.lawson@bbsrc.ac.uk

Received 20 September 2005; Accepted 3 October 2005

Published online 12 January 2006 in Wiley InterScience (www.interscience.wiley.com). DOI: 10.1002/prot.20818

TABLE I. Summary of X-Ray Data and Model Parameters for NovW

Data collection	
Cell parameters: a = b, c (Å)	59.35, 109.03
Resolution range ^a (Å)	39–1.60 (1.64–1.60)
Unique reflections	26449
Completeness ^a (%)	99.9 (99.9)
Redundancy	5.8
R _{merge} ^{a,b}	0.060 (0.362)
(I/σ(I)) ^a	25.7 (3.9)
Wilson B value (Å ²)	15.5
Refinement	
R _{cryst} ^c (based on 95% of data; %)	15.0
R _{free} ^c (based on 5% of data; %)	19.5
DPI ^d (based on R _{free} ; Å)	0.083
Residues with most favoured φ/ψ ^e (%)	95.1
RMSD bond distances (Å)	0.014
RMSD bond angles (°)	1.492
Contents of model (molecules/nonhydrogen atoms)	
Protein (residues/atoms)	199/1500
Waters	200
Sulfate	1/5
Ethylene glycol	3/12
Average temperature factors (Å ²)	
Main-chain atoms	14.6
Side-chain atoms	17.0
Waters	30.5
Sulfate	49.2
Ethylene glycol	22.8
Overall	17.6
PDB accession code	2COZ

^aThe figures in brackets indicate the values for outer resolution shell.

^b $R_{\text{merge}} = \sum (|I_j - \langle I_j \rangle|) / \sum I_j$, where I_j is the intensity of an observation of reflection j and $\langle I_j \rangle$ is the average intensity for reflection j .

^cThe R-factors R_{cryst} and R_{free} are calculated as follows: $R = \sum (|F_{\text{obs}} - F_{\text{calc}}|) / \sum |F_{\text{obs}}| \times 100$, where F_{obs} and F_{calc} are the observed and calculated structure factor amplitudes, respectively.

^dDiffraction-component precision index³⁴—an estimate of the overall coordinate errors calculated in REFMAC5.²¹

^eAs calculated using PROCHECK.²⁴

(i.e., space group $P4_32_12$ with approximate cell parameters of $a = b = 59 \text{ \AA}$, $c = 109 \text{ \AA}$), the existing preliminary 2.0 Å structure¹⁸ could be used as a starting model. After rigid body refinement to convergence, the structure was subjected to restrained refinement with REFMAC5²¹ with the inclusion of calculated hydrogen scattering from “riding” hydrogen atoms and the use of anisotropic thermal parameters. The solvent was automatically modelled and refined with ARP.²² Interactive model building with the program O²³ was used to correct errors in the model and to introduce ligands where appropriate. After the final refinement cycle, the resultant structure was evaluated using PROCHECK.²⁴ Model parameters are summarized in Table I. Atomic coordinates have been deposited in the Protein Data Bank (PDB) with the accession code 2COZ.

Results and Discussion. There is a single NovW subunit per crystallographic asymmetric unit. The final refined model contains 199 amino acids comprising residues 1–190 of the native sequence and the last nine residues of the N-terminal hexahistidine affinity tag. Thus, 17 resi-

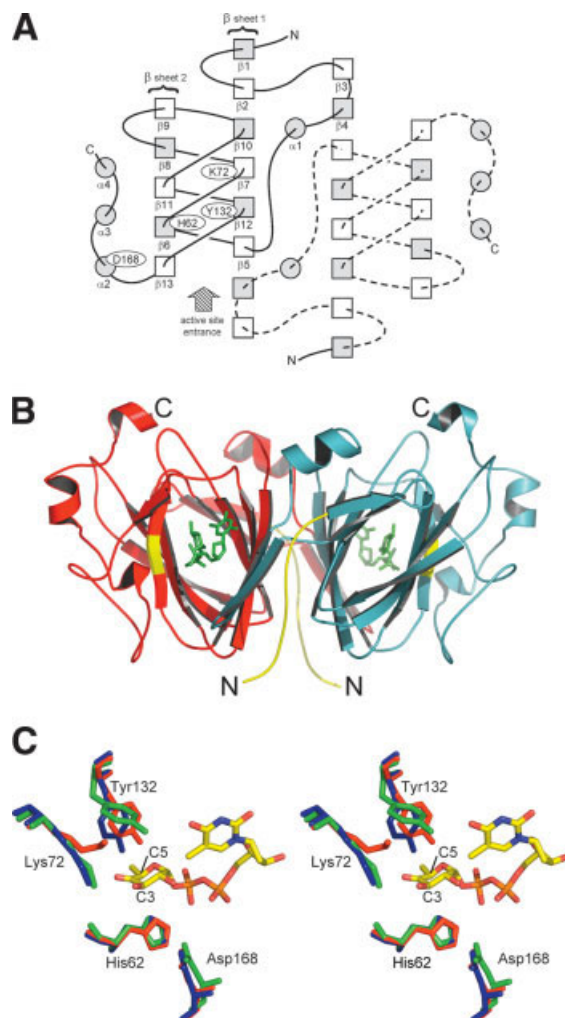


Fig 1. The structure of NovW. **A:** Topological arrangement of secondary structural elements: β -strands are represented by squares and α -helices by circles; shaded elements have their C-termini pointing toward the viewer and nonshaded elements are oriented in the opposite direction. The relative positions of key active site residues are shown and the second subunit of the dimer is indicated by dashed loop regions. **B:** Ribbon diagram showing the three-dimensional structure of homodimeric NovW. The N-terminal His tags are colored in yellow and the locations of active sites are indicated by dTDP-4-keto-6-deoxyglucose molecules shown in green. The residues forming the nonproline *cis* peptide in $\beta 6$ are also colored in yellow. Access to the active centers is from the front in the left hand subunit (red) and from behind in the right hand subunit (light blue). **C:** Stereo diagram showing a superposition of key active site residues in NovW (this work; red), *S. suis* RmlC (1NYW; green), and EvaD (1OFN; blue) with dTDP-4-keto-6-deoxyglucose docked in (based on the dTDP-glucose complex of *S. suis* RmlC, 1NYW). The numbering is according to the NovW sequence. Parts B and C were generated using PyMOL (<http://www.pymol.sourceforge.net>).³⁵

dues of the 207-residue native sequence are not resolved at the C-terminus of the structure. The subunit structure consists of a single domain of approximately 40% β -strand and 10% α -helix and thus falls into the “mainly beta” class of protein structures. At the core of the structure is a β -sandwich comprised of six- and five-stranded antiparallel β -sheets (hereafter referred to as sheets 1 and 2, respectively) [Fig. 1(A)]. In fact, the connectivity between the sheets results in a double-stranded helical arrange-

TABLE II. Summary of NovW-Related Protein Structures

Protein	Source	Identity (%)	PDB code	Resol ^a (Å)	RMSD (Å)	Tyr χ_1 (°)	Tyr ^a χ_2 (°)	Reference
NovW	<i>S. spheroides</i>	100	2C0Z	1.60	0.0	-46	71	This work
EvaD	<i>A. orientalis</i>	46	1OFN	1.50	1.3	-55 ^{a,b}	63 ^{a,b}	30
EvaD	<i>A. orientalis</i>	46	1OI6	1.40	1.3	-56 ^{a,b}	66 ^{a,b}	30
RmlC	<i>S. typhimurium</i>	38	1DZR	2.17	1.5	-35/48 ^c	54/-59 ^c	28
RmlC	<i>S. typhimurium</i>	38	1DZT	2.20	1.6	69 ^b	-84 ^b	28
RmlC	<i>M. thermoautotrophicum</i>	43	1EP0	1.50	1.5	64	-78	33
RmlC	<i>M. thermoautotrophicum</i>	43	1EPZ	1.75	1.5	64	-73	33
RmlC	<i>S. suis</i>	29	1NXM	1.30	2.3	63 ^{a,b}	-83 ^{a,b}	27
RmlC	<i>S. suis</i>	29	1NYW	1.60	2.0	66 ^{a,b}	-73 ^{a,b}	27
RmlC	<i>S. suis</i>	29	1NZC	1.80	2.0	69 ^{a,b}	-76 ^{a,b}	27
RmlC	<i>M. tuberculosis</i>	49	1PM7	2.20	0.9	66 ^b	87 ^b	31
RmlC	<i>M. tuberculosis</i>	49	1UP1	1.70	1.0	67/4 ^{a,d}	-79/19 ^{a,d}	29
RmlC	<i>P. aeruginosa</i>	40	1RTV	2.50	1.4	58 ^a	-84 ^a	To be published
RmlC	<i>S. tokodaii</i>	30	1WLT	1.90	1.2	-49/ -36 ^c	70/57 ^c	To be published

^aSide-chains normalized as recommended by PROCHECK²⁴ to give χ_2 values that differ by 180° from the original PDB file, but a structure that is chemically equivalent.

^bTorsion angles averaged over two or more subunits with similar values.

^cTorsion angles significantly different between subunits in asymmetric unit: both sets of values are given.

^dTwo conformers of the same residue.

ment of pairs of antiparallel β -strands forming a small, laterally compressed barrel: this is characteristic of the RmlC-like cupin superfamily.²⁵ NovW forms an elongated homodimer across the crystallographic two-fold axis with approximate dimensions of $77 \times 51 \times 45$ Å [Fig. 1(B)]. The equivalent β -sheets 1 from each monomer pack against one another, and each is extended by two strands provided by the N-terminus of the neighboring subunit [Fig. 1(A)]. In total, some 1545 Å² of surface area are buried per monomer at the two-fold interface, as calculated by the Protein-Protein Interaction server (<http://www.biochem.ucl.ac.uk/bsm/PP/server/>).

In addition to sharing 87% sequence identity with the equivalent enzymes from the clorobiocin (CloW)⁶ and the coumermycin A₁ (CouW)⁵ biosynthetic pathways, NovW is highly homologous in both sequence and structure to two other biosynthetic enzymes, namely, RmlC, a dTDP-6-deoxy-D-xylo-4-hexulose-3,5-epimerase from the rhamnose pathway,¹⁶ and EvaD, a dTDP-3-amino-2,3,6-trideoxy-3-C-methyl-D-erythro-hexo-4-ulose-5-epimerase from the chloreremomycin pathway.²⁶ To date, there are a total of 11 RmlC structures (derived from six different microbes) and two of EvaD (from the same microbial source) in the PDB. These are summarized in Table II. All of these are dimeric and align closely with NovW, giving root-mean-square deviations (RMSDs) in C α positions in the range 0.9–2.3 Å (for the monomer), with at least 91% of the structure overlapped.

In the NovW dimer, the axes of the two cupin barrels are approximately parallel, but inverted relative to one another. They are only open at one end to give a narrow cleft approximately 14 Å long, 3 Å across, and 12 Å deep [Fig. 1(B)]. This corresponds to the active sites defined in the RmlC and EvaD enzymes.^{27–31} Key residues implicated in the catalytic mechanisms of these two enzymes are structurally conserved in NovW, being His62, Asp168, Lys72,

and Tyr132 [Fig. 1(C)]. His62 and Asp168 form a hydrogen-bonded dyad, and it is thought that this is responsible for proton abstraction from one face of the sugar ring to give an enolate intermediate, which is stabilized by the Lys side-chain. The catalytic cycle is completed by proton donation to the opposite face by the Tyr or, possibly, a water molecule.²⁷ In RmlC, epimerization occurs at both C3 and C5, requiring two sequential catalytic cycles, whereas EvaD epimerizes only once at C5. An additional dyad, formed by His119 and Asp83, lies adjacent to the active site in NovW, and is well conserved in the RmlCs and EvaD. However, it is notably absent in *Streptococcus suis* RmlC, a validated 3,5-epimerase, and thus is not considered to be catalytically important.²⁷ It has previously been observed that the disposition of the proposed catalytic residues in the RmlC structures and EvaD is very similar; the exception is in the orientation of the Tyr.³⁰ In the majority of RmlC structures, the hydroxyl group points toward the mouth of the active site cleft (e.g. $\chi_1 = 63^\circ$, $\chi_2 = -83^\circ$ for Tyr140 in *S. suis* RmlC; PDB code 1NXM), whereas in EvaD, the direction of the hydroxyl is roughly perpendicular to that in most RmlCs, pointing across the active site cleft (e.g., $\chi_1 = -55^\circ$, $\chi_2 = 63^\circ$ for Tyr133 in *Amycolatopsis orientalis* EvaD; PDB code 1OFN) (Table II). It has subsequently been speculated that the orientation of the Tyr determines whether the enzyme is a 5-epimerase, as in EvaD, or a 3,5-epimerase, as in RmlC.³⁰ Nevertheless, conformations similar to that seen in EvaD are also observed for the equivalent Tyr side-chains in two RmlC structures (1DZR and 1WLT). Likewise, Tyr132 in NovW adopts a conformation comparable to that of EvaD ($\chi_1 = -46^\circ$, $\chi_2 = 71^\circ$), but current thinking strongly suggests it is not a 5-epimerase.^{4,17} Even though the two active sites of the dimer are on opposite faces of the molecule, the hydroxyl groups of the two Tyr132 residues are only approximately 22 Å apart. It is not known

whether there is any cooperativity in the mechanism of NovW or, indeed, in any of the related enzymes.

In RmlC-like sequences, the most conserved stretch of continuous sequence is the penta-peptide VX₁RGX₂H comprising most of β -strand 6, where the His is the catalytic base (His62 in NovW) and the Arg side-chain projects into the active site (Arg59 in NovW). The latter is implicated in substrate binding, forming hydrogen bonds to phosphate groups of bound ligands in four of the RmlC structures (1DZT, 1EPZ, 1NYW, and 1NZC); to a sulfate in NovW and *S. typhimurium* RmlC (1DZT); to a tartrate in *P. aeruginosa* RmlC (1RTV); and to glycerol in EvaD (1OFN). Both X₁ and X₂ are Leu in authentic RmlCs, but are more variable in NovW, CloW, CouW, and EvaD: X₁ varies between Val, Ile, and Leu, and X₂ can be either Val or Ile. However, the significance of this observation is unclear as the side-chains of residues X₁ and X₂ point away from the active center, and are thus unlikely to have a direct influence on substrate binding or the catalytic cycle. Also of note in this region is the G-X₂ peptide bond. In NovW, EvaD, and the majority of RmlC structures, this is built in the *cis* configuration. In the structures where this bond is not *cis* (1DZR, 1DZT, 1NZC, and 1RTV), there appears to be significant local distortion of the geometry, which could be resolved by rebuilding as *cis*.²⁹ Nonproline *cis* peptides are relatively uncommon in protein structures and frequently occur in functionally important regions³²; thus, the occurrence of this one adjacent to the active site is perhaps no coincidence. However, its role is not immediately apparent, although it has been suggested that it may be "required to orient catalytic residues found on β 6 in the active site".³³ Indeed, in NovW and EvaD, and all RmlC structures with the exception of one (1PM7), the side-chain of His62 stacks against the protein backbone of the Gly (Gly60 in NovW). From a purely structural perspective, the *cis* peptide helps to maintain the continuity of β -sheet 2. β 6 is sandwiched between β 11 and β 13, which lie at an angle of approximately 55° relative to one another, looking down the β -barrel axis [Fig. 1(B)]. The *cis* peptide puts a 25° kink into β 6 such that the N-terminal half (residues 58–60) is juxtaposed with β 11, and the C-terminal half (residues 61–64) is juxtaposed with β 13. Two further *cis* peptide bonds are present in the NovW structure, but both of these precede Pro residues. They are adjacent in sequence (Val66-Pro67 and Pro67-Pro68), lying in the surface loop connecting strands β 6 and β 7. These are only conserved in the structures of the homologs with the greatest structural similarity to NovW, namely, in EvaD (1OFN, 1O16), *M. tuberculosis* RmlC (1PM7, 1UPI), and *S. tokodaii* RmlC (1WLT; but only the first *cis* Pro is present). Thus, an important structural or functional role for this motif seems unlikely.

To further our understanding of the biological activity of NovW, we have attempted to produce complexes with potential substrates and their analogs by either cocrystallization or soaking into preexisting crystals. Thus far, this has been unsuccessful, which may be attributable to the ammonium sulfate required for the crystallization (25% saturation).¹⁸ The latter could competitively inhibit ligand

binding, because a sulfate anion is observed in the active site pocket in the crystal structure. Trials to obtain a new crystal form of NovW are underway in an attempt to circumvent this problem. Nevertheless, plausible models of the enzyme–substrate complex can be derived by manually docking dTDP-4-keto-6-deoxyglucose (the product of both NovT and RmlB, the dehydratases from the novobiocin and rhamnase pathways, respectively) into the active center with reference to the known structures of RmlC complexes, in particular that of *S. suis* with dTDP-glucose bound (1NYW). Inspection of the active sites of NovW, *S. suis* RmlC and EvaD superposed, shows that in RmlC the active site Tyr is poised over the sugar moiety, the hydroxyl being approximately equidistant from C3 and C5, whereas in NovW and EvaD, the hydroxyl points away from the sugar, being closest to C5 [Fig. 1(C)]. In the absence of a crystal structure of the complex, one cannot rule out the possibility that the conformation of Tyr132 may change upon the binding of substrate to become similar to that found in the majority of RmlC structures. Although, in general, the catalytic residues of RmlC enzymes do not reorient significantly in the cases where structures of both the apo form and ligand-bound complexes are available (Table II).

In conclusion, we have determined the high-resolution crystal structure of NovW, a homodimeric 4-keto-6-deoxy sugar epimerase from the novobiocin biosynthetic gene cluster of *S. spheroides*. It bears very significant structural similarity to the RmlC and EvaD sugar epimerases. The orientation of a strictly conserved Tyr residue in the active center is similar to that of EvaD, but distinctly different from that of the majority of RmlC structures. This residue is postulated to act as the catalytic acid in the epimerization reaction, and thus its conformation may have important mechanistic implications for NovW. Nevertheless, structural analysis alone is unlikely to answer the more subtle questions regarding the true biological activity of NovW. Therefore, we are currently using a combination of mass spectrometry, nuclear magnetic resonance spectroscopy and site-directed mutagenesis in order to firmly establish the position of NovW in the noviose biosynthetic pathway and to confirm whether it functions as a 3-mono- or a 3,5-di-epimerase.

Acknowledgments. Financial support was provided by the BBSRC (P.J., M.J.B., and D.M.L.), the Norwich Research Park (M.T.), the Weston Foundation (R.A.F.), and the National Institutes of Health grants F32 AI054007 and GM 49338 (C.L.F.M. and C.T.W., respectively). L. Heide is acknowledged for the provision of cosmid 10-9C containing the novobiocin cluster of *S. spheroides*, and the authors thank J.H. Naismith for helpful discussions.

REFERENCES

1. Maxwell A. DNA gyrase as a drug target. *Trends Microbiol* 1997;5:102–109.
2. Walsh TJ, Standiford HC, Reboli AC, et al. Randomized double-blind trial of rifampin with either novobiocin or trimethoprim-sulfamethoxazole against methicillin-resistant *Staphylococcus aureus* colonization: prevention of antimicrobial resistance and effect

- of host factors on outcome. *Antimicrob Agents Chemother* 1993;37:1334–1342.
- Montecalvo MA, Horowitz H, Wormser GP, Seiter K, Carbonaro CA. Effect of novobiocin-containing antimicrobial regimens on infection and colonization with vancomycin-resistant *Enterococcus faecium*. *Antimicrob Agents Chemother* 1995;39:794.
 - Steffensky M, Muhlenweg A, Wang ZX, Li SM, Heide L. Identification of the novobiocin biosynthetic gene cluster of *Streptomyces spheroides* NCIB 11891. *Antimicrob Agents Chemother* 2000;44:1214–1222.
 - Wang ZX, Li SM, Heide L. Identification of the coumermycin A(1) biosynthetic gene cluster of *Streptomyces rishiriensis* DSM 40489. *Antimicrob Agents Chemother* 2000;44:3040–3048.
 - Pojer F, Li SM, Heide L. Molecular cloning and sequence analysis of the clorobiocin biosynthetic gene cluster: new insights into the biosynthesis of aminocoumarin antibiotics. *Microbiology* 2002;148:3901–3911.
 - Gust B, Challis GL, Fowler K, Kieser T, Chater KF. PCR-targeted *Streptomyces* gene replacement identifies a protein domain needed for biosynthesis of the sesquiterpene soil odor geosmin. *Proc Natl Acad Sci USA* 2003;100:1541–1546.
 - Freitag A, Rapp H, Heide L, Li SM. Metabolic engineering of aminocoumarins: inactivation of the methyltransferase gene *cloP* and generation of new clorobiocin derivatives in a heterologous host. *Chembiochem* 2005;6(8):1411–1418.
 - Li SM, Heide L. New aminocoumarin antibiotics from genetically engineered *Streptomyces* strains. *Curr Med Chem* 2005;12:419–427.
 - Xu H, Heide L, Li S-M. New aminocoumarin antibiotics formed by a combined mutational and chemoenzymatic approach utilizing the carbamoyltransferase NovN. *Chem Biol* 2004;11:655–662.
 - Gellert M, O’Dea MH, Itoh T, Tomizawa J. Novobiocin and coumermycin inhibit DNA supercoiling catalyzed by DNA gyrase. *Proc Natl Acad Sci USA* 1976;73:4474–4478.
 - Maxwell A, Lawson DM. The ATP-binding site of type II topoisomerases as a target for antibacterial drugs. *Curr Top Med Chem* 2003;3:283–303.
 - Lewis RJ, Singh OM, Smith CV, et al. The nature of inhibition of DNA gyrase by the coumarins and the cyclothialidines revealed by X-ray crystallography. *EMBO J* 1996;15:1412–1420.
 - Holdgate GA, Tunnicliffe A, Ward WH, et al. The entropic penalty of ordered water accounts for weaker binding of the antibiotic novobiocin to a resistant mutant of DNA gyrase: a thermodynamic and crystallographic study. *Biochemistry* 1997;36:9663–9673.
 - Tsai FT, Singh OM, Skarzynski T, et al. The high-resolution crystal structure of a 24-kDa gyrase B fragment from *E. coli* complexed with one of the most potent coumarin inhibitors, clorobiocin. *Proteins* 1997;28:41–52.
 - Giraud MF, Naismith JH. The rhamnose pathway. *Curr Opin Struct Biol* 2000;10:687–696.
 - Thu Thuy TT, Lee HC, Kim C-G, Heide L, Sohng JK. Functional characterizations of *novWUS* involved in novobiocin biosynthesis from *Streptomyces spheroides*. *Arch Biochem Biophys* 2005;436:161–167.
 - Jakimowicz P, Freil Meyers CL, Walsh CT, Buttner MJ, Lawson DM. Crystallization and preliminary X-ray studies on the putative dTDP sugar epimerase NovW from the novobiocin biosynthetic cluster of *Streptomyces spheroides*. *Acta Crystallogr D Biol Crystallogr* 2003;59:1507–1509.
 - Otwinowski Z, Minor W. Processing of X-ray diffraction data collected in oscillation mode. *Methods Enzymol* 1997;276:307–326.
 - Collaborative Computational Project No. 4. The CCP4 suite: programs for protein crystallography. *Acta Crystallogr D Biol Crystallogr* 1994;50:760–763.
 - Murshudov GN, Vagin AA, Dodson EJ. Refinement of macromolecular structures by the maximum-likelihood method. *Acta Crystallogr D Biol Crystallogr* 1997;53:240–255.
 - Lamzin VS, Wilson KS. Automated refinement of protein models. *Acta Crystallogr D Biol Crystallogr* 1993;49:129–147.
 - Jones TA, Zou JY, Cowan SW, Kjeldgaard M. Improved methods for building protein models in electron density maps and the location of errors in these models. *Acta Crystallogr D Biol Crystallogr* 1991;47:110–119.
 - Laskowski RA, MacArthur MW, Moss DS, Thornton JM. PROCHECK: a program to check the stereochemical quality of protein structures. *J Appl Cryst* 1993;26:283–291.
 - Dunwell JM, Culham A, Carter CE, Sosa-Aguirre CR, Goodenough PW. Evolution of functional diversity in the cupin superfamily. *Trends Biochem Sci* 2001;26:740–746.
 - Chen H, Thomas MG, Hubbard BK, Losey HC, Walsh CT, Burkart MD. Deoxysugars in glycopeptide antibiotics: enzymatic synthesis of TDP-L-epivancosamine in chloroeremomycin biosynthesis. *Proc Natl Acad Sci USA* 2000;97:11942–11947.
 - Dong C, Major LL, Allen A, Blankenfeldt W, Maskell D, Naismith JH. High-resolution structures of RmlC from *Streptococcus suis* in complex with substrate analogs locate the active site of this class of enzyme. *Structure (Camb)* 2003;11:715–723.
 - Giraud MF, Leonard GA, Field RA, Bernlind C, Naismith JH. RmlC, the third enzyme of dTDP-L-rhamnose pathway, is a new class of epimerase. *Nat Struct Biol* 2000;7:398–402.
 - Kantardjieff KA, Kim CY, Naranjo C, et al. *Mycobacterium tuberculosis* RmlC epimerase (Rv3465): a promising drug-target structure in the rhamnose pathway. *Acta Crystallogr D Biol Crystallogr* 2004;60:895–902.
 - Merkel AB, Major LL, Errey JC, et al. The position of a key tyrosine in dTDP-4-keto-6-deoxy-D-glucose-5-epimerase (EvaD) alters the substrate profile for this RmlC-like enzyme. *J Biol Chem* 2004;279:32684–32691.
 - Babaoglu K, Page MA, Jones VC, et al. Novel inhibitors of an emerging target in *Mycobacterium tuberculosis*: substituted thiazolidinones as inhibitors of dTDP-rhamnose synthesis. *Bioorg Med Chem Lett* 2003;13:3227–3230.
 - Jabs A, Weiss MS, Hilgenfeld R. Non-proline cis peptide bonds in proteins. *J Mol Biol* 1999;286:291–304.
 - Christendat D, Saridakis V, Dharamsi A, et al. Crystal structure of dTDP-4-keto-6-deoxy-D-hexulose 3,5-epimerase from *Methanobacterium thermoautotrophicum* complexed with dTDP. *J Biol Chem* 2000;275:24608–24612.
 - Cruickshank DWJ. Remarks about protein structure precision. *Acta Crystallogr D Biol Crystallogr* 1999;55:583–601.
 - DeLano WL. The PyMOL user’s manual. San Carlos, CA: DeLano Scientific; 2002.